

# <sup>1</sup> The human visual system preserves the hierarchy <sup>2</sup> of 2-dimensional pattern regularity

<sup>3</sup> Peter J. Kohler<sup>1,2,3</sup> and Alasdair D. F. Clarke<sup>4</sup>

<sup>4</sup> *<sup>1</sup> York University, Department of Psychology, Toronto, ON M3J 1P3, Canada*

<sup>5</sup> *<sup>2</sup> Centre for Vision Research, York University, Toronto, ON, M3J 1P3, Canada*

<sup>6</sup> *<sup>3</sup> Stanford University, Department of Psychology, Stanford, CA 94305, United States*

<sup>7</sup> *<sup>4</sup> University of Essex, Department of Psychology, Colchester, UK, CO4 3SQ*

## <sup>8</sup> Abstract

<sup>9</sup> Symmetries are present at many scales in images of natural scenes. A large body of literature  
<sup>10</sup> has demonstrated contributions of symmetry to numerous domains of visual perception.  
<sup>11</sup> The four fundamental symmetries, reflection, rotation, translation and glide reflection, can be  
<sup>12</sup> combined in exactly 17 distinct ways. These *wallpaper groups* represent the complete set of  
<sup>13</sup> symmetries in 2D images and have recently found use in the vision science community as  
<sup>14</sup> an ideal stimulus set for studying the perception of symmetries in textures. The goal of the  
<sup>15</sup> current study is to provide a more comprehensive description of responses to symmetry in the  
<sup>16</sup> human visual system, by collecting both brain imaging (Steady-State Visual Evoked Poten-  
<sup>17</sup> tials measured using high-density EEG) and behavioral (symmetry detection thresholds) data  
<sup>18</sup> using the entire set of wallpaper groups. This allows us to probe the hierarchy of complexity  
<sup>19</sup> among wallpaper groups, in which simpler groups are subgroups of more complex ones. We  
<sup>20</sup> find that this hierarchy is preserved almost perfectly in both behavior and brain activity: A  
<sup>21</sup> multi-level Bayesian GLM indicates that for most of the 63 subgroup relationships, subgroups  
<sup>22</sup> produce lower amplitude responses in visual cortex (posterior probability: > 0.95 for 56 of 63)  
<sup>23</sup> and require longer presentation durations to be reliably detected (posterior probability: > 0.95  
<sup>24</sup> for 49 of 63). This systematic pattern is seen only in visual cortex and only in components of  
<sup>25</sup> the brain response known to be symmetric-specific. Our results show that representations of  
<sup>26</sup> symmetries in the human brain are precise and rich in detail, and that this precision is reflected  
<sup>27</sup> in behavior. These findings expand our understanding of symmetry perception, and open up  
<sup>28</sup> new avenues for research on how fine-grained representations of regular textures contribute  
<sup>29</sup> to natural vision.

<sup>30</sup> Symmetries are abundant in natural and man-made environments, due to a complex interplay  
<sup>31</sup> of physical forces that govern pattern formation in nature. Symmetrical patterns have been  
<sup>32</sup> created and appreciated by human cultures throughout history and since the gestalt movement  
<sup>33</sup> of the early 20th century, symmetry has been recognized as important for visual perception.  
<sup>34</sup> Symmetry contributes to the perception of shapes (Palmer, 1985; Li et al., 2013), scenes (Apthorp  
<sup>35</sup> and Bell, 2015) and surface properties (Cohen and Zaidi, 2013), as well as the social process of mate  
<sup>36</sup> selection (Møller, 1992). Most of this work has focused on mirror symmetry or *reflection*, with less  
<sup>37</sup> attention being paid to the other fundamental symmetries: *rotation*, *translation* and *glide reflection*

(Wagemans, 1998). This is perhaps because that reflection has been found to be more perceptually salient (Mach, 1959; Royer, 1981; Palmer, 1991; Ogden et al., 2016; Hamada and Ishihara, 1988) and produced more brain activity (Makin et al., 2013, 2014, 2012; Wright et al., 2015) than other types of symmetry. The current study considers all of the four fundamental symmetries not in isolation, but when they are combined in regular textures. In the two spatial dimensions relevant for images, symmetries can be combined in 17 distinct ways, *the wallpaper groups* (Fedorov, 1891; Polya, 1924; Liu et al., 2010). Previous work on a subset of four of the wallpaper groups used functional MRI to demonstrate that rotation symmetries in wallpapers elicit parametric responses in several areas in occipital cortex, beginning with visual area V3 (Kohler et al., 2016). This effect was also robust when symmetry responses were measured with electroencephalography (EEG) using both Steady-State Visual Evoked Potentials (SSVEPs) (Kohler et al., 2016) and Event-Related Potentials (Kohler et al., 2018). The SSVEP technique uses periodic visual stimulation to produce a periodic brain response that is confined to integer multiples of the stimulation frequency known as harmonics. SSVEP response harmonics can be isolated in the frequency domain and depending on the specific design, different harmonics will in some cases express different aspects of the brain response. (Norcia et al., 2015). Here we extend on the previous work by collecting SSVEPs and psychophysical data from human participants viewing the full set of wallpaper groups. We measure responses in visual cortex to 16 out of the 17 wallpaper groups, with the 17th serving as a control stimulus. Our goal is to provide a more complete picture of how wallpaper groups are represented in the human visual system.

A wallpaper group is a topologically discrete group of isometries of the Euclidean plane, i.e. transformations that preserve distance (Liu et al., 2010). The wallpaper groups differ in the number and kind of these transformations and we can uniquely refer to different groups using crystallographic notation. In brief, most groups are notated by  $PXZ$ , where  $X \in \{1, 2, 3, 4, 6\}$  indicates the highest order of rotational symmetry and  $Z \in \{m, g\}$  indicates whether the pattern contains mirror or glide symmetry. For example,  $P4$  contains 4 fold rotation, while  $P2M$  contains 2 fold rotation and a mirror symmetry (see Figure XXX). Two of the groups start with a  $C$  rather than a  $P$ , ( $CM$  and  $CMM$ ) which indicates that the symmetries are specified relative to a cell that itself contains repetition. Full details of the naming convention and examples of the wallpaper groups can be found on wikipedia.

In mathematical group theory, when the elements of one group is completely contained in another, the inner group is called a subgroup of the outer group (Liu et al., 2010). The full list of subgroup relationships is listed in Section 1.4.2 of the Supplementary Material. Subgroup relationships between wallpaper groups can be distinguished by their indices. The index of a subgroup relationship is the number of cosets, i.e. the number of times the subgroup is found in the supergroup (Liu et al., 2010). As an example, let us consider groups  $P_2$  and  $P_6$ . If we ignore the translations in two directions that both groups share, group  $P_6$  consists of the set of rotations  $\{0^\circ, 60^\circ, 120^\circ, 180^\circ, 240^\circ, 300^\circ\}$ , in which  $P_2 \{0^\circ, 180^\circ\}$  is contained.  $P_2$  is thus a subgroup of  $P_6$ , and  $P_6$  can be generated by combining  $P_2$  with rotations  $\{0^\circ, 120^\circ, 240^\circ\}$ . Because  $P_2$  is repeated three times in  $P_6$ ,  $P_2$  is a subgroup of  $P_6$  with index 3 (Liu et al., 2010). The 17 wallpaper groups thus obey a hierarchy of complexity where simpler groups are subgroups of more complex ones

<sup>79</sup> (Coxeter and Moser, 1972).

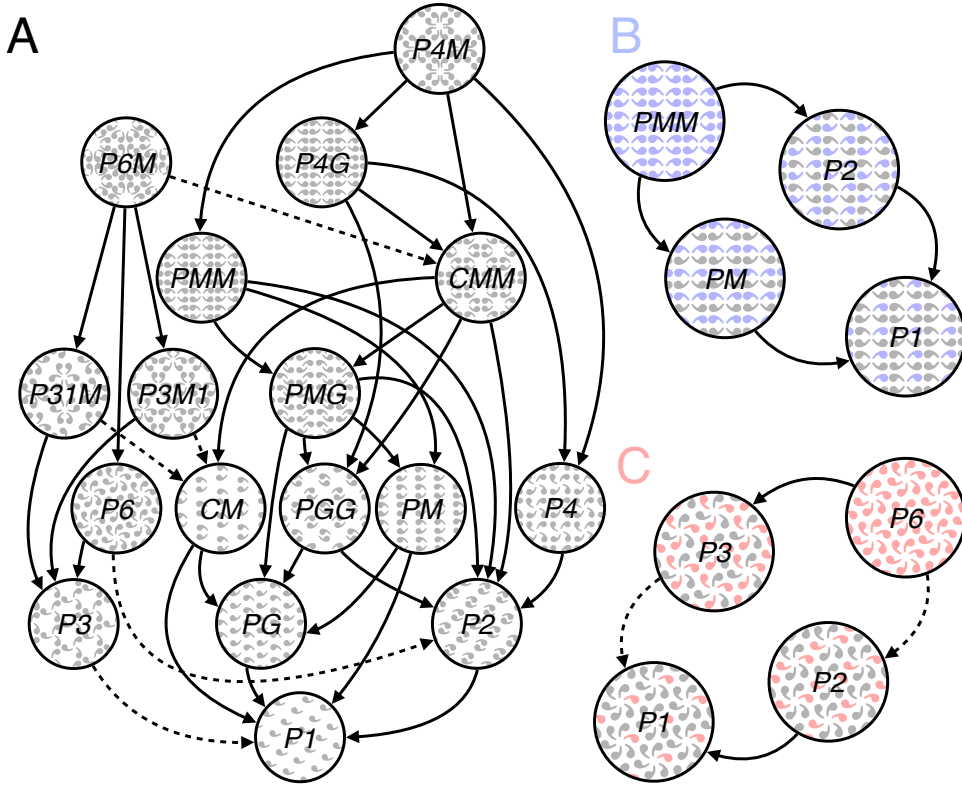


Figure 1: Subgroup relationships with indices 2 (solid lines) and 3 (dashed line) are shown in (A). All other relationships can be inferred by identifying the shortest path through the hierarchy, and multiplying the subgroup indices. For example,  $P_1$  is related to  $P_6$  through  $P_6 \rightarrow P_3$  (index 2) and  $P_3 \rightarrow P_1$  (index 3) so  $P_1$  is also a subgroup of  $P_6$  with index  $3 \times 2 = 6$ . We also show enlarged versions of some of the subgroup relationships involving  $PMM$  (B, shown in blue) and  $P6$  (C, shown in red) and highlight the symmetries within the subgroups to emphasize how the supergroup can be generated by adding additional transformations to the subgroup.

The two datasets we present here make it possible to assess the extent to which both behavior and brain responses follow the hierarchy of complexity expressed by the subgroup relationships. Based on previous brain imaging work showing that patterns with more axes of symmetry produce greater activity in visual cortex (Sasaki et al., 2005; Tyler et al., 2005; Kohler et al., 2018, 2016; Keefe et al., 2018), we hypothesized that more complex groups would produce larger SSVEPs. For the psychophysical data, we hypothesized that more complex groups would lead to shorter symmetry detection thresholds, based on previous data showing that under a fixed presentation time, discriminability increases with the number of symmetry axes in the pattern (Wagemans et al., 1991). Our results confirm both hypotheses, and show that activity in human visual cortex is remarkably consistent with the hierarchical relationships between the wallpaper groups, with SSVEP amplitudes and psychophysical thresholds following these relationships at a level that is far beyond chance. The human visual system thus appears to encode all of the fundamental symmetries using a representational structure that closely approximates the subgroup relationships from group theory.

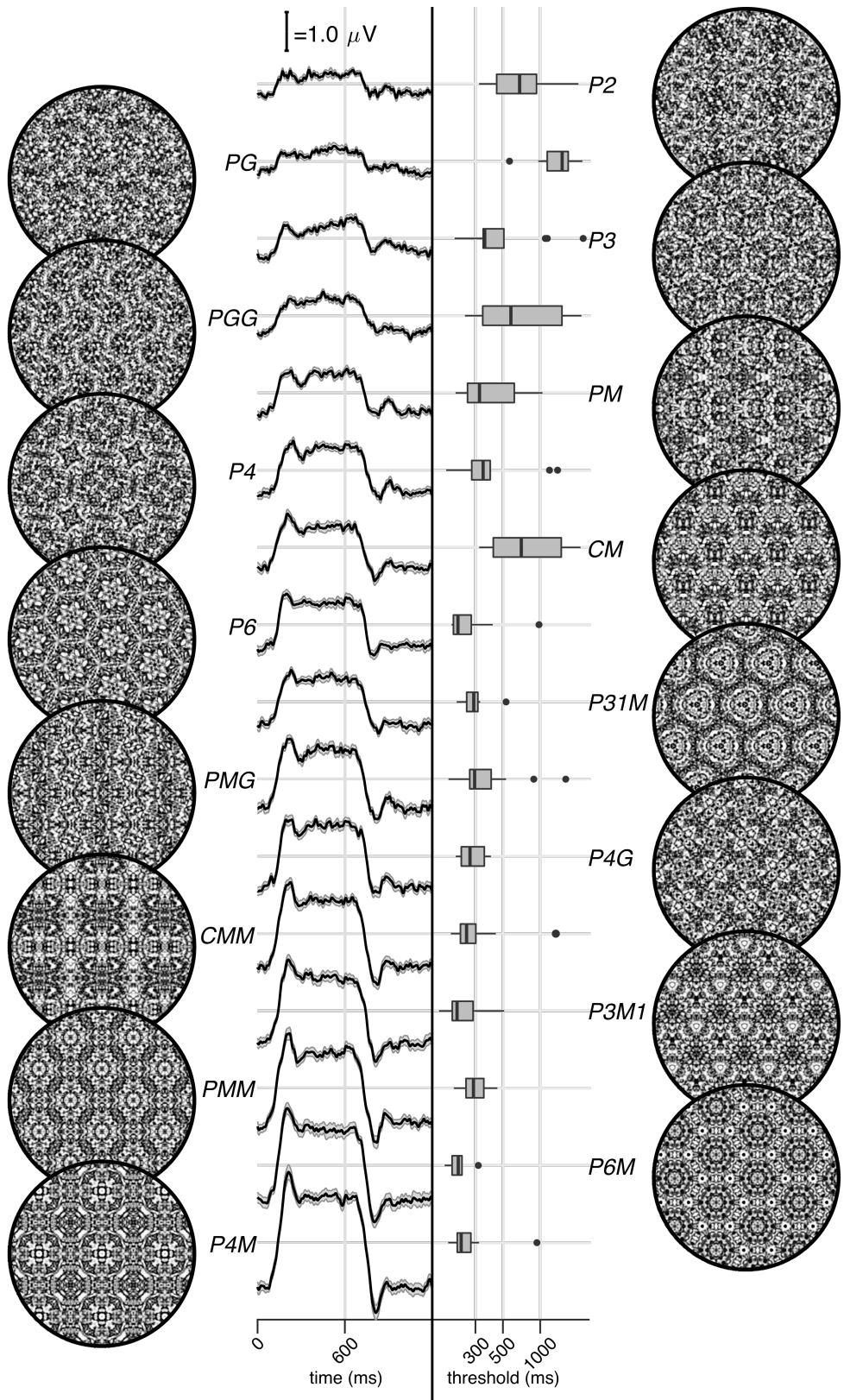


Figure 2: Examples of each of the 16 wallpaper groups are shown in the left- and right-most column of the figures, next to the corresponding SSVEP (center-left) and psychological (center-right) data from each group. The SSVEP data are odd-harmonic-filtered cycle-average waveforms. In each cycle, a  $P_1$  exemplar was shown for the first 600 ms, followed by the original exemplar for the last 600 ms. Errorbars are standard error of the mean. Psychophysical data are presented as boxplots reflecting the distribution of display duration thresholds. The 16 groups are ordered by the strength of the SSVEP response, to highlight the range of response amplitudes.

94 **Results**

95 The stimuli used in our two experiments were generated from random-noise textures, which  
96 made it possible to generate multiple exemplars from each of the wallpaper groups, as described  
97 in detail elsewhere (Kohler et al., 2016). We generated control stimuli matched to each exemplar  
98 in the main stimulus set, by scrambling the phase but maintaining the power spectrum. All  
99 wallpaper groups are inherently periodic because of their repeating lattice structure. Phase  
100 scrambling maintains this periodicity, so the phase-scrambled control images all belong to group  
101  $P_1$  regardless of group membership of the original exemplar.  $P_1$  contains no symmetries other  
102 than translation, while all other groups contain translation in combination with one or more of the  
103 other three fundamental symmetries (reflection, rotation, glide reflection) (Liu et al., 2010). In our  
104 SSVEP experiment, this stimulus set allowed us to isolate brain activity specific to the symmetry  
105 structure in the exemplar images from activity associated with modulation of low-level features,  
106 by alternating exemplar images and control exemplars. In this design, responses to structural  
107 features beyond the shared power spectrum, including any symmetries other than translation,  
108 are isolated in the odd harmonics of the image update frequency (Kohler et al., 2016; Norcia et al.,  
109 2015, 2002). Thus, the combined magnitude of the odd harmonic response components can be  
110 used as a measure of the overall strength of the visual cortex response.

111 The psychophysical experiment took a distinct but related approach. In each trial an exemplar  
112 image was shown with its matched control, one image after the other, and the order varied pseudo-  
113 randomly such that in half the trials the original exemplar was shown first, and in the other half  
114 the control image was shown first. After each trial, participants were instructed to indicate  
115 whether the first or second image contained more structure. The duration of both images was  
116 controlled by a staircase procedure so that a threshold duration for symmetry detection could be  
117 computed for each wallpaper group.

118 Examples of the wallpaper groups and a summary of our brain imaging and psychophysical  
119 measurements are shown in Figure 2. For our primary SSVEP analysis, we only considered EEG  
120 data from a pre-determined region-of-interest (ROI) consisting of six electrodes over occipital cor-  
121 tex (see Supplementary Figure 1.1). SSVEP data from this ROI was filtered so that only the odd  
122 harmonics that capture the symmetry response contribute to the waveforms. While waveform am-  
123 plitude is quite variable among the 16 groups, all groups have a sustained negative-going response  
124 that begins at about the same time for all groups, 180 ms after the transition from the  $P_1$  control  
125 exemplar to the original exemplar. To reduce the amplitude of the symmetry-specific response to  
126 a single number that could be used in further analyses and compared to the psychophysical data,  
127 we computed the root-mean-square (RMS) over the odd-harmonic-filtered waveforms. The data  
128 in Figure 2 are shown in descending order according to RMS. The psychophysical results, shown  
129 in box plots in Figure 2, were also quite variable between groups, and there seems to be a general  
130 pattern where wallpaper groups near the top of the figure, that have lower SSVEP amplitudes,  
131 also have longer psychophysical threshold durations.

132 We now wanted to test our two hypotheses about how SSVEP amplitudes and threshold du-  
133 rations would follow subgroup relationships, and thereby quantify the degree to which our two  
134 measurements were consistent with the group theoretical hierarchy of complexity. We tested

each hypothesis using the same approach. We first fitted a Bayesian model with wallpaper group as a factor and participant as a random effect. We fit the model separately for SSVEP RMS and psychophysical data and then computed posterior distributions for the difference between supergroup and subgroup. These difference distributions allowed us to compute the conditional probability that the supergroup would produce (a) larger RMS and (b) a shorter threshold durations, when compared to the subgroup. The posterior distributions are shown in Figure 3 for the SSVEP data, and in Figure 4 for the psychophysical data, which distributions color-coded according to conditional probability. For both data sets our hypothesis is confirmed: For the overwhelming majority of the 63 subgroup relationships, supergroups are more likely to produce larger symmetry-specific SSVEPs and shorter symmetry detection threshold durations, and in most cases the conditional probability of this happening is extremely high.

We also ran a control analysis using (1) odd-harmonic SSVEP data from a six-electrode ROI over parietal cortex (see Supplementary Figure 1.1) and (2) even-harmonic SSVEP data from the same occipital ROI that was used in our primary analysis. By comparing these two control analysis to our primary SSVEP analysis, we can address the specify of our effects in terms of location (occipital cortex vs parietal cortex) and harmonic (odd vs even). For both control analyses (plotted in Supplementary Figures 3.3 and 3.4), the correspondence between data and subgroup relationships was substantially weaker than in the primary analysis. We can quantify the strength of the association between the data and the subgroup relationships, by asking what proportion of subgroup relationships that reach or exceed a range of probability thresholds. This is plotted in Figure 5, for our psychophysical data, our primary SSVEP analysis and our two control SSVEP analyses. It shows that odd-harmonic SSVEP data from the occipital ROI and symmetry detection threshold durations both have a strong association with the subgroup relationships such that a clear majority of the subgroups survive even at the highest threshold we consider ( $p(\Delta > 0 | data) > 0.99$ ). The association is far weaker for the two control analyses.

SSVEP data from four of the wallpaper groups ( $P_2, P_3, P_4$  and  $P_6$ ) was previously published as part of our earlier demonstration of parametric responses to rotation symmetry in wallpaper groups (Kohler et al., 2016). We replicate that result using our Bayesian approach, and find an analogous parametric effect in the psychophysical data (see Supplementary Figure 4.1). We also conducted an analysis testing for an effect of index in our two datasets and found that subgroup relationships with higher indices tended to produce greater pairwise differences between the subgroup and supergroup, for both SSVEP RMS and symmetry detection thresholds (see Supplementary Figure 4.2). The effect of index is relatively weak, but the fact that there is a measurable index effect can nonetheless be taken as preliminary evidence that representations of symmetries in wallpaper groups may be compositional.

Finally, we conducted a correlation analysis comparing SSVEP and psychophysical data and found a reliable correlation ( $R^2 = 0.44$ , Bayesian confidence interval [0.28, 0.55]). The correlation reflects an inverse relationship: For subgroup relationships where the supergroup produces a much *larger* SSVEP amplitude than the subgroup, the supergroup also tends to produce a much *smaller* symmetry detection threshold. This is consistent with our hypotheses about how the two measurements relate to symmetry representations in the brain, and suggests that our brain

imaging and psychophysical measurements are at least to some extent tapping into the same underlying mechanisms.

## Discussion

Here we show that beyond merely responding to the elementary symmetry operations of reflection (Sasaki et al., 2005; Tyler et al., 2005) and rotation (Kohler et al., 2016), the visual system represents the hierarchical structure of the 17 wallpaper groups, and thus every composition of the four fundamental symmetries (rotation, reflection, translation, glide reflection) which comprise the set of regular textures. Both SSVEP amplitudes and symmetry detection thresholds preserve the hierarchy of complexity among the wallpaper groups that is captured by the subgroup relationships (Coxeter and Moser, 1972). For the SSVEP, this remarkable consistency was specific to the odd harmonics of the stimulus frequency that are known to capture the symmetry-specific response (Kohler et al., 2016) and to electrodes in a region-of-interest (ROI) over occipital cortex. When the same analysis was done using the odd harmonics from electrodes over parietal cortex (Supplementary Figure 3.3) or even harmonics from electrodes over occipital cortex (Supplementary Figure 3.4), the data was substantially less consistent with the subgroup relationships (yellow and green lines, Figure 5).

The current study uses 16 distinct wallpaper groups, while previous neuroimaging studies focused on a subset of 4 (Kohler et al., 2016, 2018). This represents a significant conceptual advance, because it makes it possible to investigate the complete subgroup hierarchy among the 17 groups and ask to what extent the hierarchy is reflected in brain activity. Our data provide a description of the visual system's response to the complete set of symmetries in the two-dimensional plane. We do not independently measure the response to  $P_1$ , but because each of the 16 other groups produce non-zero odd harmonic amplitudes (see Figure 2), we can conclude that the relationships between  $P_1$  and all other groups, where  $P_1$  is the subgroup, are also preserved by the visual system. The subgroup relationships are in many cases not obvious perceptually, and most participants had no knowledge of group theory. Thus, the visual system's ability to preserve the subgroup hierarchy does not depend on explicit knowledge of the relationships. Previous brain-imaging studies have found evidence of parametric responses with the number of reflection symmetry folds (Keefe et al. (2018); Sasaki et al. (2005); Makin et al. (2016) and with the order of rotation symmetry (Kohler et al. (2016)). Our study is the first demonstration that the brain encodes symmetry in this parametric fashion across every possible combination of different symmetry types, and that this parametric encoding is also reflected in behavior. Previous behavioral experiments have shown that although naïve observers can distinguish many of the wallpaper groups (Landwehr, 2009), they tend to sort exemplars into fewer (4-12) sets than the number of wallpaper groups, often placing exemplars from different wallpaper groups in the same set (Clarke et al., 2011). The two-interval forced choice approach we use in the current psychophysical experiment makes it possible to directly compare symmetry detection thresholds to the subgroup hierarchy, and reveals that not only can the 17 wallpaper groups be distinguished based on behavioral data, behavior largely follows the subgroup hierarchy.

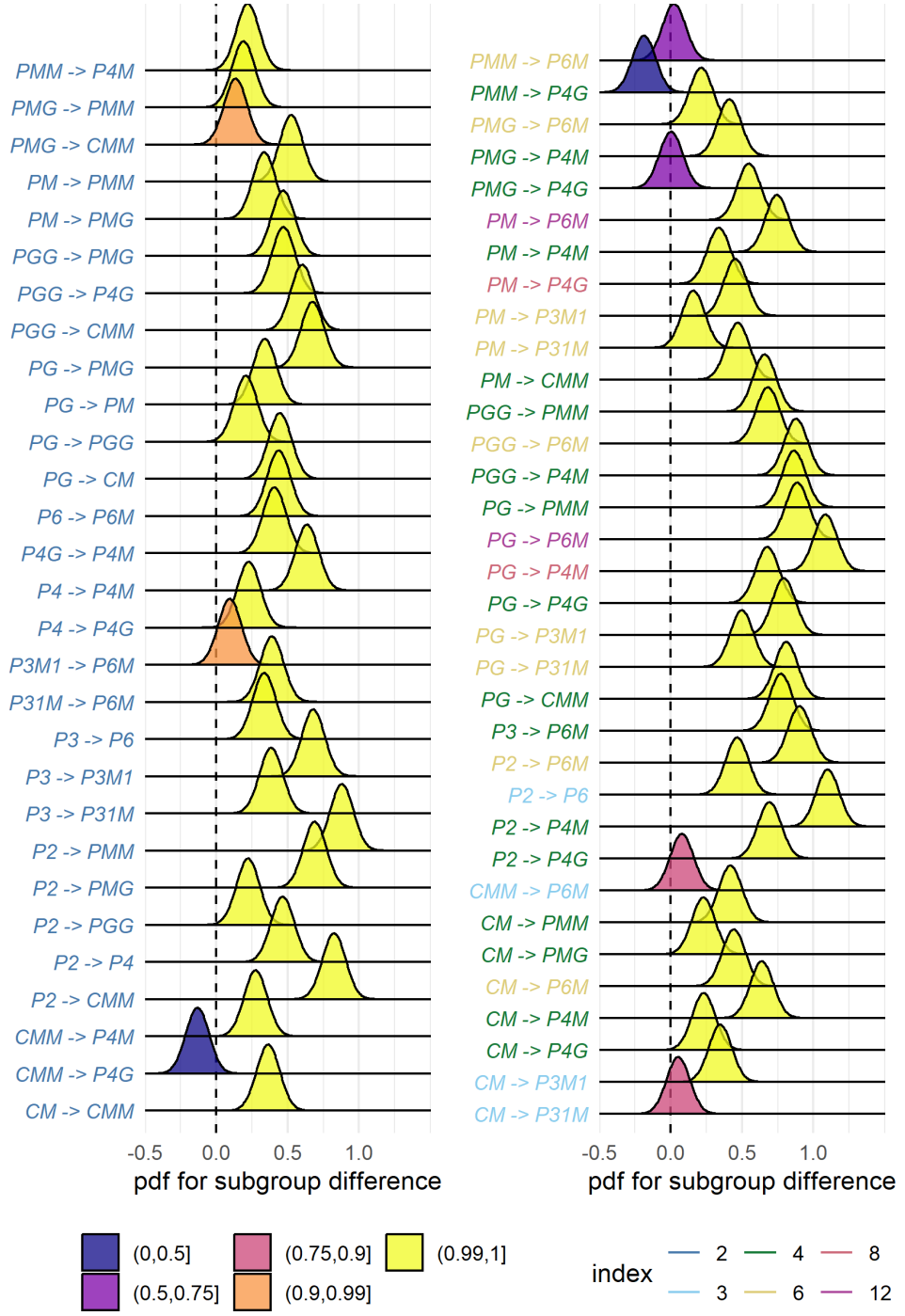


Figure 3: Posterior distributions for the difference in mean SSVEP RMS amplitude. Colour coding of the text indicates the index of the subgroup, while the colour of the filled distribution relates to the conditional probability that the difference in means is greater than zero. We can see that 55/63 subgroup relationships have  $p(\Delta|data) > 0.99$ .

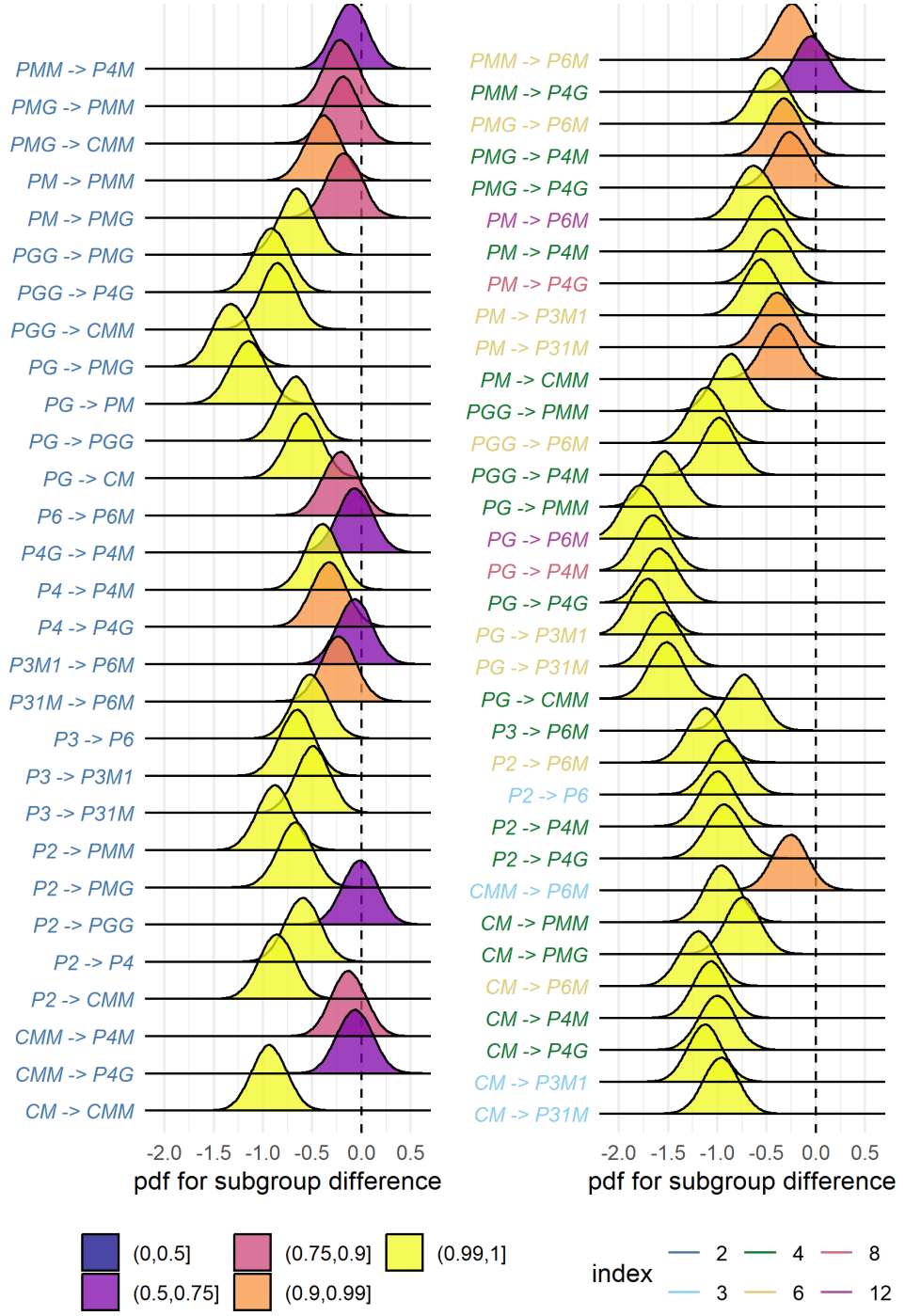


Figure 4: Posterior distributions for the difference in mean symmetry detection threshold durations. Colour coding of the text indicates the index of the subgroup, while the colour of the filled distribution relates to the conditional probability that the difference in means is greater than zero. We can see that 43/63 subgroup relationships have  $p(\Delta|data) > 0.99$ .

215 A large literature exists on the *Sustained Posterior Negativity* (SPN), a characteristic negative-  
216 going waveform that is known to reflect responses to symmetry and other forms of regularity  
217 and structure (Makin et al., 2016). The SPN scales with the proportion of reflection symmetry  
218 in displays that contain a mixture of symmetry and noise Makin et al. (2020); Palumbo et al.  
219 (2015), and both reflection, rotation and translation can produce a measurable SPN Makin et al.  
220 (2013). It has recently been demonstrated that a holographic model of regularity (van der Helm  
221 and Leeuwenberg, 1996), can predict both SPN amplitude (Makin et al., 2016) and perceptual  
222 discrimination performance (Nucci and Wagemans, 2007) for dot patterns that contain symmetry  
223 and other types of regularity. The available evidence suggests that the SPN and our SSVEP  
224 measurements are two distinct methods of isolating the same symmetry-related brain response:  
225 When observed in the time-domain, the symmetry-selective odd-harmonic responses produce  
226 similarly sustained waveforms (see Figure 2), odd-harmonic SSVEP responses can be measured  
227 for dot patterns similar to those used to measure the SPN (Norcia et al., 2002), and the one event-  
228 related study that has been published on the wallpaper groups also produced SPN-like waveforms  
229 (Kohler et al., 2018). Future work should more firmly establish the connection and determine if  
230 the SPN can capture responses similarly precise symmetry responses as the SSVEPs presented  
231 here. It would also be worthwhile to ask if and how  $W$  can be computed for our random-noise based  
232 wallpaper textures where combinations of symmetries tile the plane.

233 We observe a reliable correlation between our brain imaging and psychophysical data. This  
234 suggests that the two measurements reflect the same underlying symmetry representations in  
235 visual cortex. It should be noted that the correlation is relatively modest ( $R^2 = 0.44$ ). This may  
236 be partly due to the fact that different individuals participated in the two experiments. It may  
237 also be related to the fact that participants were not doing a symmetry-related task during the  
238 SSVEP experiment, but instead monitored the stimuli for brief changes in contrast that occurred  
239 twice per trial (see Methods). Previous brain imaging studies have found enhanced reflection  
240 symmetry responses when participants performed a symmetry-related task Makin et al. (2020);  
241 Sasaki et al. (2005); Keefe et al. (2018). We did not manipulate task during our SSVEP recordings,  
242 but it is possible that adding a symmetry-related task to our SSVEP experiment would have  
243 produced measurements that reflected subgroup relationships to an even higher extent. We  
244 note, however, that our performance is already close to ceiling (see Figure 5). It is possible that  
245 adding a symmetry-related task would enhance SSVEP amplitudes across all wallpaper groups  
246 without improving the discriminability of individual groups (similar to what was observed by Keefe  
247 and his co-authors Keefe et al. (2018)). SPN measurements suggest that task-driven processing  
248 may be important for detecting symmetries that have been subject to perspective distortion  
249 Makin et al. (2015) although it should be noted that this effect was much less clear in a subsequent  
250 functional MRI study Keefe et al. (2018). Future work in which behavioral and brain imaging  
251 data are collected from the same participants, and behavior is manipulated in the SSVEP task, will  
252 help further establish the connection between the two measurements, and elucidate the potential  
253 contribution of task-related top-down processing to the current results.

254 We also find an effect of index for both our brain imaging measurements and our symmetry  
255 detection thresholds. This means that the visual system not only represents the hierarchical rela-

tionship captured by individual subgroups, but also distinguishes between subgroups depending on how many times the subgroup is repeated in the supergroup, with more repetitions leading to larger pairwise differences. Our measured effect of index is relatively weak. This is perhaps because the index analysis does not take into account the *type* of isometries that differentiate the subgroup and supergroup. The effect of symmetry type can be observed by contrasting the measured SSVEP amplitudes and detection thresholds for groups *PM* and *PG* in Figure 2. The two groups are comparable except *PM* contains reflection and *PG* contains glide reflection, and the former clearly elicits higher amplitudes and lower thresholds. An important goal for future work will be to map out how different symmetry types contribute to the representational hierarchy.

The correspondence between responses in the visual system and group theory that we demonstrate here, may reflect a form of implicit learning that depends on the structure of the natural world. The environment is itself constrained by physical forces underlying pattern formation and these forces are subject to multiple symmetry constraints (Hoyle, 2006). The ordered structure of responses to wallpaper groups could be driven by a central tenet of neural coding, that of efficiency. If coding is to be efficient, neural resources should be distributed to capture the structure of the environment with minimum redundancy considering the visual geometric optics, the capabilities of the subsequent neural coding stages and the behavioral goals of the organism (At-tneave, 1954; Barlow, 1961; Laughlin, 1981; Geisler et al., 2009). Early work within the efficient coding framework suggested that natural images had a  $1/f$  spectrum and that the corresponding redundancy between pixels in natural images could be coded efficiently with a sparse set of oriented filter responses, such as those present in the early visual pathway (Field, 1987; Olshausen and Field, 1997). Our results suggest that the principle of efficient coding extends to a much higher level of structural redundancy – that of symmetries in visual images.

The 17 wallpaper groups are completely regular, and relatively rare in the visual environment, especially when considering distortions due to perspective (see above) and occlusion. Near-regular textures, however, abound in the visual world, and can be modeled as deformed versions of the wallpaper groups (Liu et al., 2004). The correspondence between visual cortex responses and group theory demonstrated here may indicate that the visual system represents visual textures using a similar scheme, with the wallpaper groups serving as anchor points in representational space. This framework resembles norm-based encoding strategies that have been proposed for other stimulus classes, most notably faces (Leopold et al., 2006), and leads to the prediction that adaptation to wallpaper patterns should distort perception of near-regular textures, similar to the aftereffects found for faces (Webster and MacLin, 1999). Field biologists have demonstrated that animals respond more strongly to exaggerated versions of a learned stimulus, referred to as “supernormal” stimuli (Tinbergen, 1953). In the norm-based encoding framework, wallpaper groups can be considered *supertextures*, exaggerated examples of the near-regular textures that surround us. Artists may consciously or unconsciously create supernormal stimuli, to capture the essence of the subject and evoke strong responses in the audience (Ramachandran and Hirstein, 1999). Wallpaper groups are visually compelling, and symmetries have been widely used in human artistic expression going back to the Neolithic age (Jablan, 2014). If wallpapers are in fact supertextures, this prevalence may be a direct result of the strategy the human visual system has

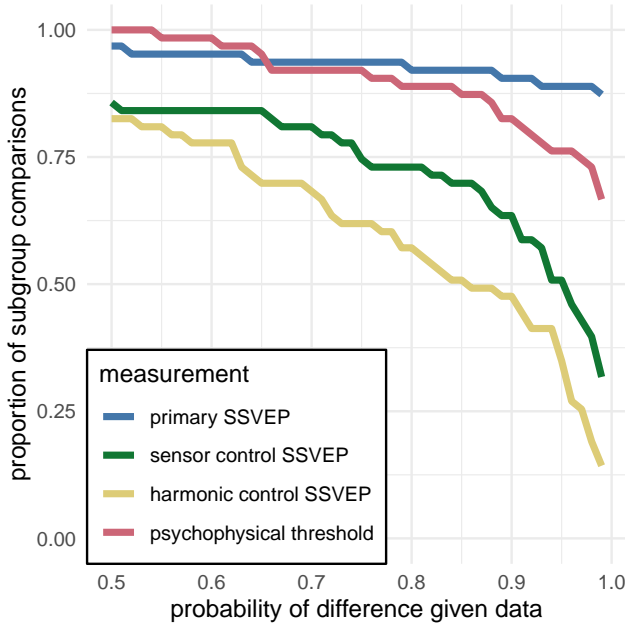


Figure 5: This plot shows the proportion of subgroup relationships that satisfy  $p(\Delta > 0 | data) > x$ . We can see that if we take  $x = 0.95$  as our threshold, the subgroup relationships are preserved in  $56/63 = 89\%$  and  $48/63 = 76\%$  of the comparisons for the primary SSVEP and threshold duration datasets, respectively. This compares to the  $32/63 = 51\%$  and  $22/63 = 35\%$  for the SSVEP control datasets.

297 adopted for texture encoding.

## 298 Participants

299 Twenty-five participants (11 females, mean age  $28.7 \pm 3.3$ ) took part in the EEG experiment.  
300 Their informed consent was obtained before the experiment under a protocol that was approved  
301 by the Institutional Review Board of Stanford University. 11 participants (8 females, mean age  
302  $20.73 \pm 1.21$ ) took part in the psychophysics experiment. All participants had normal or corrected-to-normal vision. Their informed consent was obtained before the experiment under a protocol  
303 that was approved by the University of Essex's Ethics Committee. **There was no overlap in**  
304 **participants between the EEG and psychophysics experiments.**

## 306 Stimulus Generation

307 Exemplars from the different wallpaper groups were generated using a modified version of the  
308 methodology developed by Clarke and colleagues (Clarke et al., 2011) that we have described in de-  
309 tail elsewhere (Kohler et al., 2016). Briefly, exemplar patterns for each group were generated from  
310 random-noise textures, which were then repeated and transformed to cover the plane, according  
311 to the symmetry axes and geometric lattice specific to each group. The use of noise textures as  
312 the starting point for stimulus generation allowed the creation of an almost infinite number of  
313 distinct exemplars of each wallpaper group. To make individual exemplars as similar as possible  
314 we replaced the power spectrum of each exemplar with the median across exemplars within a

group. We then generated control exemplars that had the same power spectrum as the exemplar images by randomizing the phase of each exemplar image. The phase scrambling eliminates rotation, reflection and glide-reflection symmetries within each exemplar, but the phase-scrambled images inherit the spectral periodicity arising from the periodic tiling. This means that all control exemplars, regardless of which wallpaper group they are derived from, are transformed into another symmetry group, namely  $P_1$ .  $P_1$  is the simplest of the wallpaper groups and contains only translations of a region whose shape derives from the lattice. Because the different wallpaper groups have different lattices,  $P_1$  controls matched to different groups have different power spectra. Our experimental design takes these differences into account by comparing the neural responses evoked by each wallpaper group to responses evoked by the matched control exemplars.

## Stimulus Presentation

Stimulus Presentation. For the EEG experiment, the stimuli were shown on a 24.5" Sony Trimension EL PVM-2541 organic light emitting diode (OLED) display at a screen resolution of  $1920 \times 1080$  pixels, 8-bit color depth and a refresh rate of 60 Hz, viewed at a distance of 70 cm. The mean luminance was  $69.93\text{ cd/m}^2$  and contrast was 95%. The diameter of the circular aperture in which the wallpaper pattern appeared was  $13.8^\circ$  of visual angle presented against a mean luminance gray background. Stimulus presentation was controlled using in-house software. For the psychophysics experiment, the stimuli were shown on a  $48 \times 27\text{cm}$  VIEWPixx/3D LCD Display monitor, model VPX-VPX-2005C, resolution  $1920 \times 1080$  pixels, with a viewing distance of approximately 40cm and linear gamma. Stimulus presentation was controlled using MatLab and Psychtoolbox-3 (Kleiner et al., 2007; Brainard, 1997). The diameter of the circular aperture for the stimuli was  $21.5^\circ$ .

## EEG Procedure

Visual Evoked Potentials were measured using a steady-state design, in which  $P_1$  control images alternated with exemplar images from each of the 16 other wallpaper groups. Exemplar images were always preceded by their matched  $P_1$  control image. A single  $0.83\text{ Hz}$  stimulus cycle consisted of a control  $P_1$  image followed by an exemplar image, each shown for 600 ms. A trial consisted of 10 such cycles (12 sec) over which 10 different exemplar images and matched controls from the same rotation group were presented. For each group type, the individual exemplar images were always shown in the same order within the trials. Participants initiated each trial with a button-press, which allowed them to take breaks between trials. Trials from a single wallpaper group were presented in blocks of four repetitions, which were themselves repeated twice per session, and shown in random order within each session. To control fixation, the participants were instructed to fixate a small white cross in the center of display. To control vigilance, a contrast dimming task was employed. Two times per trial, an image pair ([control  \$P\_1\$  plus exemplar](#)) was shown at reduced contrast. Participants were instructed to press a button on a response pad [whenever they noticed a contrast change](#). [Reaction times were not taken into account and participants were told to respond at their own pace while being as accurate as possible](#). We adjusted the [reduction in contrast](#) such that average accuracy for each participant was kept at 85% correct, in order to

354 keep the difficulty of the vigilance task at a constant level.

## 355 Psychophysics Procedure

356 The experiment consisted of 16 blocks, one for each of the wallpaper groups (excluding  $P_1$ ). We  
357 used a two-interval forced choice approach. In each trial, participants were presented with two  
358 stimuli (one of which was the wallpaper group for the current block of trials, the other being  $P_1$ ),  
359 one after the other (inter-stimulus interval of 700ms). After each stimulus had been presented, it  
360 was masked with white noise for 300ms. After both stimuli had been presented, participants made  
361 a response on the keyboard to indicate whether they thought the first or second image contained  
362 more symmetry. Each block started with 10 practice trials, (stimulus display duration of 500ms)  
363 to allow participants to familiarise themselves with the current block's wallpaper pattern. If they  
364 achieved an accuracy of 9/10 in these trials they progressed to the rest of the block, otherwise  
365 they carried out another set of 10 practise trials. This process was repeated until the required  
366 accuracy of 9/10 was obtained. The rest of the block consisted of four interleaved staircases (using  
367 the QUEST algorithm (Watson and Pelli, 1983), full details given in the SI) of 30 trials each. On  
368 average, a block of trials took around 10 minutes to complete.

## 369 EEG Acquisition and Preprocessing

370 Steady-State Visual Evoked Potentials (SSVEPs) were collected with 128-sensor HydroCell Sensor  
371 Nets (Electrical Geodesics, Eugene, OR) and were band-pass filtered from 0.3 to 50 Hz. Raw data  
372 were evaluated off line according to a sample-by-sample thresholding procedure to remove noisy  
373 sensors that were replaced by the average of the six nearest spatial neighbors. On average, less  
374 than 5% of the electrodes were substituted; these electrodes were mainly located near the forehead  
375 or the ears. The substitutions can be expected to have a negligible impact on our results, as the  
376 majority of our signal can be expected to come from electrodes over occipital, temporal and parietal  
377 cortices. After this operation, the waveforms were re-referenced to the common average of all  
378 the sensors. The data from each 12s trial were segmented into five 2.4 s long epochs (i.e., each of  
379 these epochs was exactly 2 cycles of image modulation). Epochs for which a large percentage of  
380 data samples exceeding a noise threshold (depending on the participant and ranging between 25  
381 and 50  $\mu$ V) were excluded from the analysis on a sensor-by-sensor basis. This was typically the  
382 case for epochs containing artifacts, such as blinks or eye movements. Steady-state stimulation  
383 will drive cortical responses at specific frequencies directly tied to the stimulus frequency. It is  
384 thus appropriate to quantify these responses in terms of both phase and amplitude. Therefore, a  
385 Fourier analysis was applied on every remaining epoch using a discrete Fourier transform with a  
386 rectangular window. The use of two-cycle long epochs (i.e., 2.4 s) was motivated by the need to  
387 have a relatively high resolution in the frequency domain,  $\delta f = 0.42$  Hz. For each frequency bin,  
388 the complex-valued Fourier coefficients were then averaged across all epochs within each trial.  
389 Each participant did two sessions of 8 trials per condition, which resulted in a total of 16 trials  
390 per condition.

391 SSVEP Analysis

392 Response waveforms were generated for each group by selective filtering in the frequency do-  
393 main. For each participant, the average Fourier coefficients from the two sessions were averaged  
394 over trials and sessions. The SSVEP paradigm we used allowed us to separate symmetry-related  
395 responses from non-specific contrast transient responses. Previous work has demonstrated that  
396 symmetry-related responses are predominantly found in the odd harmonics of the stimulus fre-  
397 quency, whereas the even harmonics consist mainly of responses unrelated to symmetry, that  
398 arise from the contrast change associated with the appearance of the second image (Norcia et al.,  
399 2002; Kohler et al., 2016). This functional distinction of the harmonics allowed us to generate  
400 a single-cycle waveform containing the response specific to symmetry, by filtering out the even  
401 harmonics in the spectral domain, and then back-transforming the remaining signal, consisting  
402 only of odd harmonics, into the time-domain. For our main analysis, we averaged the odd har-  
403 monic single-cycle waveforms within a six-electrode region of interest (ROI) over occipital cortex  
404 (electrodes 70, 74, 75, 81, 82, 83). These waveforms, averaged over participants, are shown in  
405 Figure 2. The same analysis was done for the even harmonics and for the odd harmonics within a  
406 six electrode ROI over parietal cortex (electrodes 53, 54, 61, 78, 79, 86; see Supplementary Figure  
407 1.1). The root-mean square values of these waveforms, for each individual participant, were used  
408 to determine whether each of the wallpaper subgroup relationships were preserved in the brain  
409 data.

410 Defining the list of subgroup relationships

411 In order to get the complete list of subgroup relationships, we digitized Table 4 from Coxeter  
412 (Coxeter and Moser, 1972) (shown in Supplementary Table 1.2). After removing identity rela-  
413 tionships (i.e. each group is a subgroup of itself) and the three pairs of wallpaper groups that are  
414 subgroups of each other (e.g. *PM* is a subgroup of *CM*, and *CM* is a subgroup of *PM*) we were left  
415 with a total of 63 unambiguous subgroups that were included in our analysis.

416 Bayesian Analysis of SSVEP and Psychophysical data

417 Bayesian analysis was carried out using R (v3.6.1) (R Core Team, 2019) with the **brms** package  
418 (v2.9.0) (Bürkner, 2017) and rStan (v2.19.2 (Stan Development Team, 2019)). The data from each  
419 experiment were modelled using a Bayesian generalised mixed effect model with wallpaper group  
420 being treated as a 16-level factor, and random effects for participant. The SSVEP data and sym-  
421 metry detection threshold durations were modelled using log-normal distributions with weakly  
422 informative,  $\mathcal{N}(0, 2)$ , priors. After fitting the model to the data, samples were drawn from the  
423 posterior distribution of the two datasets, for each wallpaper group. These samples were then  
424 recombined to calculate the distribution of differences for each of the 63 pairs of subgroup and  
425 supergroup. These distributions were then summarised by computing the conditional probabil-  
426 ity of obtaining a positive (negative) difference,  $p(\Delta|\text{data})$ . For further technical details, please  
427 see the Supplementary Materials where the full R code, model specification, prior and posterior  
428 predictive checks, and model diagnostics, can be found.

## 429 References

- 430 Apthorp, D. and Bell, J. (2015). Symmetry is less than  
431 meets the eye. *Current Biology*, 25(7):R267–R268.
- 432 Attneave, F. (1954). Some informational aspects of  
433 visual perception. *Psychol Rev*, 61(3):183–93.
- 434 Barlow, H. B. (1961). *Possible principles underlying the  
435 transformations of sensory messages*, pages 217–234.  
436 MIT Press.
- 437 Brainard, D. H. (1997). Spatial vision. *The psy-  
438 chophysics toolbox*, 10:433–436.
- 439 Bürkner, P.-C. (2017). Advanced bayesian multilevel  
440 modeling with the r package brms. *arXiv preprint  
441 arXiv:1705.11123*.
- 442 Clarke, A. D. F., Green, P. R., Halley, F., and  
443 Chantler, M. J. (2011). Similar symmetries: The  
444 role of wallpaper groups in perceptual texture sim-  
445 ilarity. *Symmetry*, 3(4):246–264.
- 446 Cohen, E. H. and Zaidi, Q. (2013). Symmetry in con-  
447 text: Salience of mirror symmetry in natural pat-  
448 terns. *Journal of vision*, 13(6).
- 449 Coxeter, H. S. M. and Moser, W. O. J. (1972). *Ge-  
450ometrators and relations for discrete groups*. Ergebnisse  
451 der Mathematik und ihrer Grenzgebiete ; Bd. 14.  
452 Springer-Verlag, Berlin, New York.
- 453 Fedorov, E. (1891). Symmetry in the plane. In *Za-  
454 piski Imperatorskogo S. Peterburgskogo Mineralogichesko-  
455 g Obshchestva [Proc. S. Peterb. Mineral. Soc.]*, volume 2,  
456 pages 345–390.
- 457 Field, D. J. (1987). Relations between the statistics  
458 of natural images and the response properties of  
459 cortical cells. *J Opt Soc Am A*, 4(12):2379–94.
- 460 Geisler, W. S., Najemnik, J., and Ing, A. D. (2009). Opti-  
461 mal stimulus encoders for natural tasks. *Journal  
462 of Vision*, 9(13):17–17.
- 463 Hamada, J. and Ishihara, T. (1988). Complexity and  
464 goodness of dot patterns varying in symmetry. *Psy-  
465 chological Research*, 50(3):155–161.
- 466 Hoyle, R. B. (2006). *Pattern formation: an introduction  
467 to methods*. Cambridge University Press.
- 468 Jablan, S. V. (2014). *Symmetry, Ornament and Modular-  
469 ity*. World Scientific Publishing Co Pte Ltd, Singa-  
470 pore, SINGAPORE.
- 471 Keefe, B. D., Gouws, A. D., Sheldon, A. A., Vernon,  
472 R. J. W., Lawrence, S. J. D., McKeefry, D. J., Wade,  
473 A. R., and Morland, A. B. (2018). Emergence of  
474 symmetry selectivity in the visual areas of the  
475 human brain: fMRI responses to symmetry pre-  
476 sented in both frontoparallel and slanted planes.  
477 *Human Brain Mapping*, 39(10):3813–3826.
- 478 Kleiner, M., Brainard, D., Pelli, D., Ingling, A., Mur-  
479 ray, R., and Broussard, C. (2007). What's new in  
480 psychtoolbox-3. *Perception*, 36:1–16.
- 481 Kohler, P. J., Clarke, A., Yakovleva, A., Liu, Y., and  
482 Norcia, A. M. (2016). Representation of maximally  
483 regular textures in human visual cortex. *The Jour-  
484 nal of Neuroscience*, 36(3):714–729.
- 485 Kohler, P. J., Cottereau, B. R., and Norcia, A. M.  
486 (2018). Dynamics of perceptual decisions about  
487 symmetry in visual cortex. *NeuroImage*, 167(Sup-  
488 plement C):316–330.
- 489 Landwehr, K. (2009). Camouflaged symmetry. *Per-  
490 ception*, 38:1712–1720.
- 491 Laughlin, S. (1981). A simple coding procedure en-  
492 hances a neuron's information capacity. *Z Natur-  
493 forsch C*, 36(9-10):910–2.
- 494 Leopold, D. A., Bondar, I. V., and Giese, M. A.  
495 (2006). Norm-based face encoding by single neu-  
496 rons in the monkey inferotemporal cortex. *Nature*,  
497 442(7102):572–5.
- 498 Li, Y., Sawada, T., Shi, Y., Steinman, R., and Pizlo, Z.  
499 (2013). *Symmetry Is the sine qua non of Shape*, book sec-  
500 tion 2, pages 21–40. Advances in Computer Vision  
and Pattern Recognition. Springer London.
- 501 Liu, Y., Hel-Or, H., Kaplan, C. S., and Van Gool,  
502 L. (2010). Computational symmetry in computer  
503 vision and computer graphics. *Foundations and  
504 Trends® in Computer Graphics and Vision*, 5(1–2):1–  
505 195.
- 506 Liu, Y., Lin, W.-C., and Hays, J. (2004). Near-regular  
507 texture analysis and manipulation. In *ACM Trans-*

- 509 actions on Graphics (TOG), volume 23, pages 368<sub>549</sub>  
 510 376. ACM.<sub>550</sub>
- 511 Mach, E. (1959). The Analysis of Sensations (1897<sub>532</sub>  
 512 English transl., Dover, New York.<sub>551</sub>
- 513 Makin, A. D. J., Rampone, G., and Bertamini, M. (2015). Conditions for view invariance in the neural response to visual symmetry. *Psychophysiology*, 52(4):532–543. eprint<sub>557</sub>  
 517 <https://onlinelibrary.wiley.com/doi/pdf/10.1111/psyp.12365>.<sub>558</sub>
- 518 Makin, A. D. J., Rampone, G., Morris, A., and Bertamini, M. (2020). The Formation of Symmetrical Gestalts Is Task-Independent, but Can Be Enhanced by Active Regularity Discrimination. *Journal of Cognitive Neuroscience*, 32(2):353–366.<sub>562</sub>
- 523 Makin, A. D. J., Rampone, G., Pecchinenda, A., and Bertamini, M. (2013). Electrophysiological responses to visuospatial regularity. *Psychophysiology*, 50(10):1045–1055. eprint<sub>567</sub>  
 527 <https://onlinelibrary.wiley.com/doi/pdf/10.1111/psyp.12082>.<sub>568</sub>
- 528 Makin, A. D. J., Rampone, G., Wright, A., Martincic, J., and Bertamini, M. (2014). Visual symmetry in objects and gaps. *Journal of Vision*, 14(3):1271–12. Publisher: The Association for Research in Vision and Ophthalmology.<sub>573</sub>
- 533 Makin, A. D. J., Wilton, M. M., Pecchinenda, A., and Bertamini, M. (2012). Symmetry perception and affective responses: A combined EEG/EMG study. *Neuropsychologia*, 50(14):3250–3261.<sub>577</sub>
- 537 Makin, A. D. J., Wright, D., Rampone, G., Palumbo, L., Guest, M., Sheehan, R., Cleaver, H., and Bertamini, M. (2016). An Electrophysiological Index of Perceptual Goodness. *Cerebral Cortex*, 26(12):4416–4434.<sub>582</sub>
- 542 Møller, A. P. (1992). Female swallow preference for symmetrical male sexual ornaments. *Nature*, 357(6375):238–240.<sub>584</sub>
- 545 Norcia, A. M., Appelbaum, L. G., Ales, J. M., Cottereau, B. R., and Rossion, B. (2015). The steady-state visual evoked potential in vision research: A review. *Journal of Vision*, 15(6):4–44.<sub>586</sub>
- 550 Norcia, A. M., Candy, T. R., Pettet, M. W., Vildavski, V. Y., and Tyler, C. W. (2002). Temporal dynamics of the human response to symmetry. *Journal of Vision*, 2(2):132–139.
- 553 Nucci, M. and Wagemans, J. (2007). Goodness of Regularity in Dot Patterns: Global Symmetry, Local Symmetry, and Their Interactions. *Perception*, 36(9):1305–1319. Publisher: SAGE Publications Ltd STM.
- 558 Ogden, R., Makin, A. D. J., Palumbo, L., and Bertamini, M. (2016). Symmetry Lasts Longer Than Random, but Only for Brief Presentations. *i-Perception*, 7(6):2041669516676824. Publisher: SAGE Publications.
- 563 Olshausen, B. A. and Field, D. J. (1997). Sparse coding with an overcomplete basis set: a strategy employed by v1? *Vision Res*, 37(23):3311–25.
- 568 Palmer, S. E. (1985). The role of symmetry in shape perception. *Acta Psychologica*, 59(1):67–90.
- 573 Palmer, S. E. (1991). Goodness, Gestalt, groups, and Garner: Local symmetry subgroups as a theory of figural goodness. In *The perception of structure: Essays in honor of Wendell R. Garner*, pages 23–39. American Psychological Association, Washington, DC, US.
- 577 Palumbo, L., Bertamini, M., and Makin, A. (2015). Scaling of the extrastriate neural response to symmetry. *Vision Research*, 117:1–8.
- 582 Polya, G. (1924). Xii. Über die analogie der kristallsymmetrie in der ebene. *Zeitschrift für Kristallographie-Crystalline Materials*, 60(1):278–282.
- 586 R Core Team (2019). *R: A Language and Environment for Statistical Computing*. R Foundation for Statistical Computing, Vienna, Austria.
- 588 Ramachandran, V. S. and Hirstein, W. (1999). The science of art: A neurological theory of aesthetic experience. *Journal of Consciousness Studies*, 6(6–7):15–41.
- 592 Royer, F. L. (1981). Detection of symmetry. *Journal of Experimental Psychology: Human Perception and Performance*, 7(6):1186–1210.

- 590 Sasaki, Y., Vanduffel, W., Knutsen, T., Tyler, C., and  
591 Tootell, R. (2005). Symmetry activates extrastriate  
592 visual cortex in human and nonhuman primates.  
593 *Proceedings of the National Academy of Sciences of the*  
594 *United States of America*, 102(8):3159–3163.
- 595 Stan Development Team (2019). RStan: the R interface  
596 face to Stan. R package version 2.19.2.
- 597 Tinbergen, N. (1953). *The herring gull's world: a study*  
598 *of the social behaviour of birds*. Frederick A. Praeger  
599 Inc., Oxford, England.
- 600 Tyler, C. W., Baseler, H. A., Kontsevich, L. L.,  
601 Likova, L. T., Wade, A. R., and Wandell, B. A.  
602 (2005). Predominantly extra-retinotopic cortical  
603 response to pattern symmetry. *Neuroimage*,  
604 24(2):306–314.
- 605 van der Helm, P. A. and Leeuwenberg, E. L. J. (1996).  
606 Goodness of visual regularities: A nontransforma-  
607 tional approach. *Psychological Review*, 103(3):420–  
608 456. Publisher: American Psychological Associa-  
609 tion.
- 613 614 616 617 619 620 624 625 626 627 628 629
- Wagemans, J. (1998). Parallel visual processes in symmetry perception: Normality and pathology. *Documenta Ophthalmologica*, 95(3):359.
- Wagemans, J., Van Gool, L., and d'Ydewalle, G. (1991). Detection of symmetry in tachistoscopically presented dot patterns: effects of multiple axes and skewing. *Perception & Psychophysics*, 50(5):413–27.
- Watson, A. B. and Pelli, D. G. (1983). Quest: A bayesian adaptive psychometric method. *Perception & Psychophysics*, 33(2):113–120.
- Webster, M. A. and MacLin, O. H. (1999). Figural aftereffects in the perception of faces. *Psychon Bull Rev*, 6(4):647–53.
- Wright, D., Makin, A. D. J., and Bertamini, M. (2015). Right-lateralized alpha desynchronization during regularity discrimination: Hemispheric specialization or directed spatial attention? *Psychophysiology*, 52(5):638–647. eprint: <https://onlinelibrary.wiley.com/doi/pdf/10.1111/psyp.12399>.